

Cite this: *Green Chem.*, 2014, **16**, 2706

# Efficient ligand-free Hiyama cross-coupling reaction catalyzed by functionalized SBA-15-supported Pd nanoparticles†

Shao-Hsien Huang,<sup>a</sup> Chun-Hsia Liu<sup>a</sup> and Chia-Min Yang<sup>\*a,b</sup>

A ligand-free Hiyama cross-coupling reaction catalyzed by functionalized SBA-15-supported Pd catalysts has been developed. The catalysts were prepared by depositing Pd nanoparticles preferentially in the micropores of the SBA-15 with hydrophobic trimethylsilyl or triphenylsilyl groups grafted on the mesopores. The nanocomposite catalysts showed excellent activities for the cross-coupling between various aryltriethoxysilanes and aryl halides under relatively mild (at 100 °C in air) reaction conditions. Moreover, the hydrophobic functionalization rendered the catalysts reusable without showing significant activity loss. The decreased activity after successive catalytic runs was attributed to a low level of Pd-leaching and a gradual collapse of mesopores of host silica. The cross-coupling protocol with the designed catalysts would be practical for use as an economical synthetic method for the construction of biphenyl derivatives.

Received 26th January 2014,  
Accepted 16th February 2014

DOI: 10.1039/c4gc00141a

www.rsc.org/greenchem

## Introduction

The Hiyama cross-coupling reaction, a palladium-catalyzed carbon-carbon bond formation between organosilanes and organohalides or their equivalents, is one of the effective methods for constructing asymmetrical biphenyls or multi-substituted alkenes that are structural components of various pharmaceuticals and other functional materials.<sup>1–6</sup> In comparison with Stille coupling using toxic tin reagents and Suzuki coupling with problems in purifying the boron reagents, the Hiyama coupling uses relatively stable, low-toxicity and easily prepared organosilanes that, after reaction, may facily convert to relatively harmless silica waste, making the coupling reactions more attractive from the environmental point of view.<sup>1–6</sup> However, the Hiyama coupling is generally catalyzed by Pd complexes containing phosphine ligands that are often toxic, air-sensitive and expensive.<sup>7–20</sup> It has therefore been of great interest to develop (phosphine) ligand-free Pd catalysts for Hiyama coupling.<sup>21–36</sup>

In addition to homogeneous catalysts, metallic Pd and Pd-containing nanoparticles have been explored as heterogeneous

catalysts for the Hiyama coupling<sup>37–46</sup> and other organic syntheses.<sup>47–51</sup> The first example was reported by Rothenberg and coworkers using bimetallic core-shell Ni-Pd nanoclusters to catalyze the coupling of phenyltrimethoxysilane and haloarenes.<sup>37</sup> After that, several research groups also tried to use Pd nanoparticles to catalyze the same type of reactions under ligand-free conditions.<sup>27–29</sup> However, the usage of the colloidal metal nanoparticles has problems of catalyst separation and recycling. These problems may be overcome by immobilizing or supporting Pd nanoparticles on/in dendrimers,<sup>40,41</sup> carbon-based materials,<sup>38,42–44</sup> or metal oxides.<sup>39,45,46</sup> As far as catalyst support is concerned, ordered mesoporous silicas (OMSs) are highly attractive mainly because of their chemical stability, high surface area for high metal dispersion, nanometer-sized porosity to facilitate molecular diffusion, and versatile surface functionalization. In comparison with OMSs, carbon-based supports can also be made with high surface area but it is generally difficult to disperse Pd or other metals on these supports because of their hydrophobic nature. Nevertheless, the adsorption of reactants on carbon supports is promoted by van der Waals interactions, leading to favorable reactant/product mass transport. Herein we report functionalized SBA-15-supported Pd catalysts for efficient and ligand-free Hiyama coupling reactions. Mesoporous SBA-15 silica is a special type of OMSs with hexagonally arranged channel-type mesopores and additional micropores in the silica walls.<sup>52–57</sup> We selectively functionalized the mesopores with hydrophobic groups,<sup>58–62</sup> aiming not only to deposit Pd nanoparticles preferentially in the hydrophilic micropores of SBA-15,<sup>58,60</sup> but also to facilitate the

<sup>a</sup>Department of Chemistry, National Tsing Hua University, Hsinchu 30013, Taiwan

<sup>b</sup>Frontier Research Center on Fundamental and Applied Sciences of Matters, National Tsing Hua University, Hsinchu 30013, Taiwan. E-mail: cmyang@mx.nthu.edu.tw;

Fax: +886-3-5165521; Tel: +886-3-5731282

†Electronic supplementary information (ESI) available: <sup>1</sup>H and <sup>13</sup>C NMR data and spectra of biphenyl products of cross-coupling reactions. See DOI: 10.1039/c4gc00141a

transport of hydrophobic reactants and prevent possible reactions of silica walls with fluoride ions and/or other additives. The designed Pd catalysts exhibited excellent activities for Hiyama coupling between various aryltriethoxysilanes and aryl halides (mainly bromides) at 100 °C in air. Moreover, a low level of Pd-leaching was observed during the coupling reaction, allowing recycling of the catalysts for the construction of biphenyl derivatives.

## Experimental

### Catalyst preparation and characterization

Mesoporous SBA-15 silica was synthesized at 60 °C by following the procedure reported previously using tetraethoxysilane as a silica source and a triblock poly(ethylene oxide)–poly(propylene oxide)–poly(ethylene oxide) copolymer Pluronic P-123 ( $\text{EO}_{20}\text{PO}_{70}\text{EO}_{20}$ ) as a structure directing agent.<sup>52,53</sup> The as-synthesized SBA-15 was stirred in aqueous solution of sulfuric acid (45 wt%) at 95 °C for 24 h to selectively vacate the mesopores.<sup>56,57</sup> The dried acid-treated SBA-15 samples were then stirred in toluene solution of trimethylchlorosilane at room temperature for 1 h or in pyridine solution of triphenylchlorosilane at 120 °C for 12 h in order to graft the open mesopores with trimethylsilyl (TMS) or triphenylsilyl (TPS) groups.<sup>61</sup> Subsequently, the samples were heated in air at 250 °C to remove the EO fragments remaining in the micropores,<sup>56,57</sup> resulting in samples referred to as M-SBA-15 (grafted with TMS groups) and P-SBA-15 (grafted with TPS groups).

To incorporate Pd nanoparticles into the functionalized SBA-15, 0.2 g M-SBA-15 or P-SBA-15 was impregnated with 0.2 mL acetone solution of dichlorobis(acetonitrile)palladium ( $\text{PdCl}_2(\text{MeCN})_2$ ), prepared by dissolving 25 mg  $\text{PdCl}_2(\text{MeCN})_2$  in 1.0 mL acetone. After drying at 60 °C, the sample was heated in hydrogen flow at 300 °C ( $1\text{ °C min}^{-1}$  heating ramp) for 3 h to reduce the metal. The resulting Pd-containing samples are designated as Pd@M-SBA-15 and Pd@P-SBA-15. A reference catalyst was also prepared by using the pure-silica SBA-15 prepared by directly heating the acid-treated SBA-15 at 250 °C (referred to as PS-S15) as a support for Pd deposition. The reference catalyst is designated as Pd@PS-S15.

Inductively coupled plasma-mass spectroscopy (ICP-MS) data were obtained using a Perkin-Elmer SCIEX-ELAN 5000 device. Powder X-ray diffraction (PXRD) data were obtained on a Mac Science 18MPX diffractometer using  $\text{Cu K}\alpha$  radiation. Nitrogen physisorption isotherms were measured at 77 K using a Quantachrome Autosorb-1-MP instrument. The isotherms were analyzed by the nonlocal density functional theory (NLDFT) method to evaluate pore sizes using the kernel of NLDFT equilibrium capillary condensation isotherms of nitrogen at 77 K on silica (adsorption branch, assuming cylindrical pore geometry). BET surface areas were calculated from adsorption branches in the relative pressure range of 0.05–0.20. Total pore volumes were evaluated at a relative pressure of 0.95. Solid-state  $^{29}\text{Si}$  MAS and  $^{13}\text{C}$  CP/MAS NMR spectra were measured on a Bruker DSX400WB spectrometer

using 4 mm MAS probes at a spinning rate of 6.5 kHz. Transmission electron microscopy (TEM) images were taken on a FEI Tecnai 20 electron microscope operated at 200 kV and a field-emission JEOL JEM-3000F electron microscope operated at 300 kV and equipped with a high-angle annular dark field detector and an energy dispersion X-ray (EDX) spectrometer.

### Catalyst activity testing

In a typical reaction, a mixture of aryl halide (0.50 mmol), aryltriethoxysilane (1.0 mmol), tetra-*n*-butylammonium fluoride trihydrate ( $\text{TBAF}\cdot 3\text{H}_2\text{O}$ , 1.0 mmol), acetic acid ( $\text{AcOH}$ , 0.50 mmol), toluene (3.0 mL) and Pd@M-SBA-15 (26 mg, or 0.5 mol% of Pd) was stirred at 100 °C under an air atmosphere for 24 h. Alternatively, 0.5 mol% of Pd@P-SBA-15 or a commercial carbon-supported Pd/C catalyst (5.4 mg, 5 wt%, Acros) was used as a catalyst. The mixture was cooled down to room temperature and then passed through a Celite pad to remove the catalyst. The filtrate was mixed with ethyl acetate ( $\text{EtOAc}$ ) and water and was then extracted repeatedly with  $\text{EtOAc}$ . The organic phase was dried over  $\text{MgSO}_4$  and the solvent was removed under reduced pressure. The residue was purified by column chromatography on silica gel (eluent: *n*-hexane– $\text{EtOAc}$ ). The obtained products were pure, and their  $^1\text{H}$  and  $^{13}\text{C}$  NMR spectra data (recorded on a Bruker 300 NMR spectrometer with  $\text{CDCl}_3$ ) were in agreement with authentic compounds.

## Results and discussion

The SBA-15 materials had an ordered 2D-hexagonal structure and exhibited the 10, 11, and 20 reflections in its small-angle PXRD pattern shown in Fig. 1a. The cell parameter *a* is 10.6 nm, which remained unchanged after subsequent treatments and metal deposition (*cf.* Fig. 1a). The sulfuric acid treatment vacated the mesopores of SBA-15,<sup>56,57</sup> as indicated by the  $\text{N}_2$  physisorption isotherms of the treated samples (*cf.* Fig. 1b) showing a sharp step with an H1-type hysteresis loop corresponding to the filling of uniform mesopores with open cylindrical geometry. The mesopore diameter of the acid-treated SBA-15 is 7.3 nm and is identical to that of PS-S15 (pure-silica sample with further 250 °C treatment). Subsequently, the mesopore surface was grafted with TMS or TPS groups and the micropores were vacated by heat treatment at 250 °C.<sup>58–61</sup> The stepwise removal of P-123 from the as-synthesized SBA-15 and surface functionalization were confirmed by  $^{13}\text{C}$  CP/MAS and  $^{29}\text{Si}$  MAS NMR.<sup>56–60</sup> Fig. 2 shows the  $^{29}\text{Si}$  MAS NMR spectra of M-SBA-15 and P-SBA-15 exhibiting the Q lines ( $\text{Q}^n$ :  $\text{Si}(\text{OSi})_n(\text{OH})_{4-n}$ ,  $n = 2\text{--}4$ , at  $-90$  to  $-112$  ppm) from SBA-15 silica and T lines attributed to the silicon atoms of TMS (14 ppm) or TPS ( $-18$  ppm) groups. The intensity ratios of the T and Q lines for the two samples are 9 : 100 and 8 : 100. The presence of TMS or TPS groups made the effective mesopore diameters slightly smaller and the values derived from  $\text{N}_2$  physisorption are 7.2 nm and 7.1 nm, respectively. Both

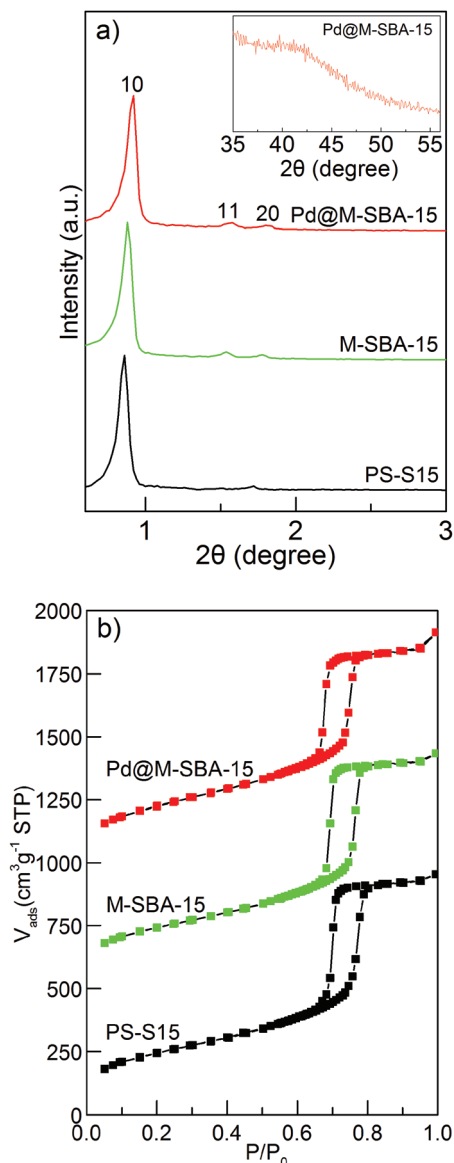


Fig. 1 PXRD patterns (a) and  $N_2$  physisorption isotherms (b) of PS-S15, M-SBA-15 and Pd@M-SBA-15. The inset in (a): wide-angle PXRD pattern of Pd@M-SBA-15. The isotherms in (b) are shifted by (from bottom to top) 0, 500 and  $1000 \text{ cm}^3 \text{ g}^{-1} \text{ STP}$ , respectively.

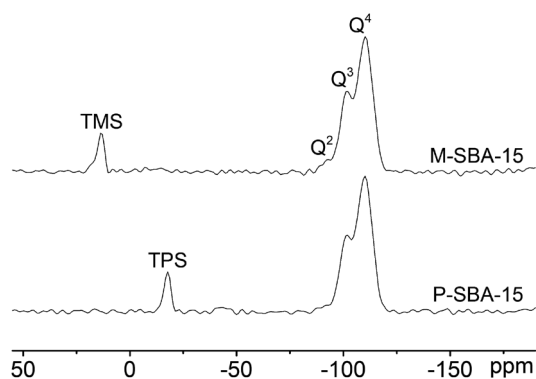


Fig. 2  $^{29}\text{Si}$  MAS NMR spectra of M-SBA-15 and P-SBA-15.

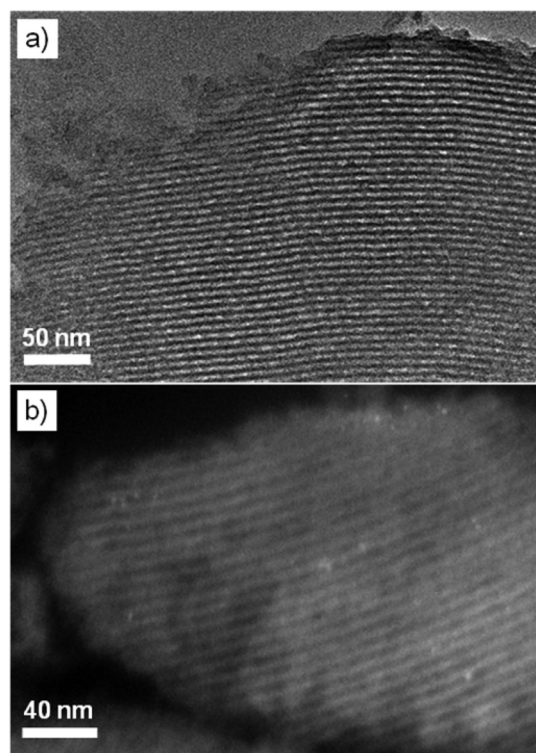


Fig. 3 Bright-field (a) and dark-field (b) TEM images of Pd@M-SBA-15.

samples had total pore volumes of around  $1.10 \text{ cm}^3 \text{ g}^{-1}$  and BET surface areas of  $740 \text{ cm}^2 \text{ g}^{-1}$ .

The samples M-SBA-15 and P-SBA-15 were applied to prepare Pd catalysts by impregnation with  $\text{PdCl}_2(\text{MeCN})_2$  followed by hydrogen reduction. The Pd loadings were 0.88 wt% (0.08 mmol Pd per gram of catalyst) determined by ICP-MS. The salt could be preferentially loaded into the micropores owing to the micropore-induced capillary forces<sup>61,62</sup> and possible interactions between the salt and surface silanol groups on micropores.<sup>58</sup> After hydrogen reduction, the samples gave featureless wide-angle PXRD patterns and show only slight changes in mesopore diameter (6.9 nm), total pore volume ( $1.06 \text{ cm}^3 \text{ g}^{-1}$ ) and surface area ( $725 \text{ cm}^2 \text{ g}^{-1}$ ) (cf. Fig. 1 for the data of Pd@M-SBA-15), indicating that the reduced Pd nanoparticles were very small without blocking the mesopores. TEM investigation was consistent with PXRD results. Fig. 3 shows the bright-field (BF) and dark-field (DF) TEM images of Pd@M-SBA-15. While fully open mesopores and no discernable Pd nanoparticles are observed in the BF image, rather inhomogeneous and highly dispersed bright contrast in the walls of mesopores observed in the DF image could be related to the Pd nanoparticles, considering that Pd is appreciably heavier than the other constituent elements. Semiquantitative analysis by EDX was in agreement with the ICP-MS result.

The SBA-15-supported Pd catalysts were used as catalysts for the Hiyama coupling reaction. We first screened the reaction conditions by performing the coupling between 4-bromoacetophenone and phenyltriethoxysilane using Pd@M-SBA-15 as a catalyst, and the results are shown in Table 1. Under the

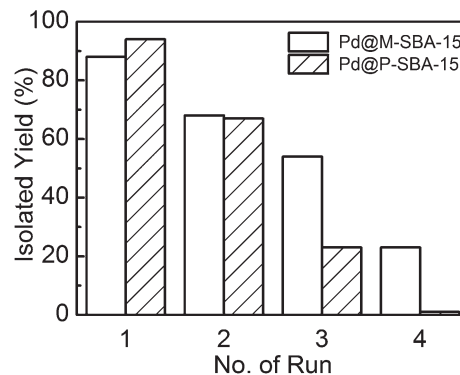
**Table 1** Optimization of reaction conditions and comparison of different catalysts<sup>a</sup>

Entry	Modified conditions	Yield <sup>b</sup> (%)
1	Standard conditions	55
2	THF instead of toluene	36
3	<i>p</i> -Xylene instead of toluene	14
4	Acetonitrile instead of toluene	4
5	Ethanol instead of toluene	4
6	KF instead of TBAF·3H <sub>2</sub> O	0
7	CsF instead of TBAF·3H <sub>2</sub> O	0
8	With 0.75 mmol of AcOH	88
9	With 0.50 mmol of AcOH	92
10	With 0.25 mmol of AcOH	74
11	Pd@P-SBA-15 was used	90
12	Pd@PS-S15 was used	56
13	5% Pd/C was used	64
14	0.05 mol% Pd@M-SBA-15	94
15	0.02 mol% Pd@M-SBA-15	3

<sup>a</sup> Under standard conditions, the reaction was carried out using Pd@M-SBA-15 (0.5 mol%, 2.5 μmol), 4-bromoacetophenone (0.50 mmol), phenyltriethoxysilane (1.0 mmol), TBAF·3H<sub>2</sub>O (1.0 mmol), and toluene (3.0 mL) in air at 100 °C for 24 h. <sup>b</sup> Isolated yields.

“standard” conditions with toluene as a solvent, the corresponding 4-acetobiphenyl was obtained in 55% isolated yield after 24 h in air at 100 °C (Table 1, entry 1). The reaction progress was affected markedly by the solvent. The desired product was obtained in moderate yield in THF (entry 2), and the reaction hardly took place in *p*-xylene, acetonitrile or ethanol (entries 3–5). For the coupling reaction, a fluoride source is necessary to activate organosilane and, as an activator, TBAF·3H<sub>2</sub>O was specifically effective probably due to its high solubility in toluene. The reaction did not proceed under fluoride-free conditions or in the presence of metal fluorides such as KF and CsF (entries 6 and 7).

On the other hand, it has been reported that the addition of AcOH as a proton source may improve the yield of the biphenyl product by suppressing the undesired coupling of the ethoxide anion (generated from phenyltriethoxysilane) with aryl halide.<sup>13,42,63</sup> Under the reaction conditions studied, the addition of AcOH indeed enhanced the reaction (entries 8–10) and an isolated yield of 92% was obtained with an amount of 1.0 equiv. of AcOH. With AcOH (1.0 equiv.), the use of Pd@P-SBA-15 gave a similar yield (entry 11) whereas the reaction catalyzed by Pd@PS-S15 resulted in a significantly lower yield of 56% (entry 12). The higher catalytic activities of Pd@M-SBA-15 and Pd@P-SBA-15 may be associated with the presence of TMS or TPS groups on the mesopores that may facilitate the diffusion of relatively hydrophobic reactants into the pore system to approach Pd nanoparticles in the intra-wall

**Fig. 4** Reuse tests of Pd@M-SBA-15 and Pd@P-SBA-15. Reaction conditions: 4-bromoacetophenone (0.50 mmol), phenyltriethoxysilane (1.0 mmol), Pd catalyst (2.5 μmol), TBAF·3H<sub>2</sub>O (1.0 mmol), AcOH (0.5 mmol), and toluene (3.0 mL) in air at 100 °C for 24 h.

micropores of SBA-15. Compared to the commercial Pd/C catalyst that gave a yield of 64% (entry 13), Pd@M-SBA-15 and Pd@P-SBA-15 were more efficient catalysts for the Hiyama coupling. Noticeably, the usage of Pd@M-SBA-15 could be markedly reduced from 0.5 mol% to 0.05 mol% with a similar yield of 4-acetobiphenyl (entry 14). It might be presumably due to the suppression of homo-coupling of the aryl bromide.<sup>42</sup> Further reduction to 0.02 mol% led to a dramatic decrease in product yield (entry 15).

The reuse tests of Pd@M-SBA-15 and Pd@P-SBA-15 (0.5 mol%) using 4-bromoacetophenone and phenyltriethoxysilane as substrates were then examined under the optimal reaction conditions (Table 1, entry 9), and after each reaction the catalyst was collected by centrifugation, filtered, dried and then reused in the next run. As shown in Fig. 4, both catalysts could be reused and the catalytic activities decreased slightly in the second run. The isolated yield of 4-acetobiphenyl remained acceptably high (54%) for Pd@M-SBA-15 in the third run but decreased to 23% in the fourth run. Nevertheless, the reaction efficiency of Pd@P-SBA-15 was already reduced drastically in the third run, which might probably be related to higher tendency for the C(sp<sup>2</sup>)-Si bonds in TPS groups to be cleaved by fluoride ions as compared to the C(sp<sup>3</sup>)-Si bonds in TMS groups.<sup>64</sup> Generally speaking, the decreased product yield after successive runs might be attributed either to the leaching of Pd species or to gradual collapse of mesopores of host silica to block the access of reactants to Pd nanoparticles. The solid catalyst was filtered after the first run of reactions and the filtrate was analyzed by ICP-MS. A Pd-leaching of 5.3 ppm was detected, which was much lower than that (60 ppm) reported for 5% Pd/C under similar reaction conditions (in the presence of AcOH).<sup>42</sup> The low level of Pd-leaching might be associated with the favorable hydrophilic environment in the micropores of SBA-15 for keeping the ionic Pd species produced during the catalytic cycle from diffusing out to the relatively hydrophobic reaction media.

We further performed a hot filtration test, in order to examine the catalytic activity of the leached Pd species, by



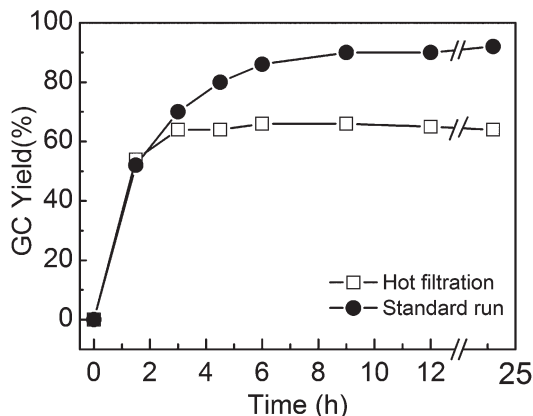


Fig. 5 Profiles of product yield versus time with or without hot filtration. Reaction conditions: 4-bromoacetophenone (0.50 mmol), phenyltriethoxysilane (1.0 mmol), Pd@M-SBA-15 (5.0  $\mu$ mol), TBAF·3H<sub>2</sub>O (1.0 mmol), AcOH (0.5 mmol), and toluene (3.0 mL) in air at 100 °C.

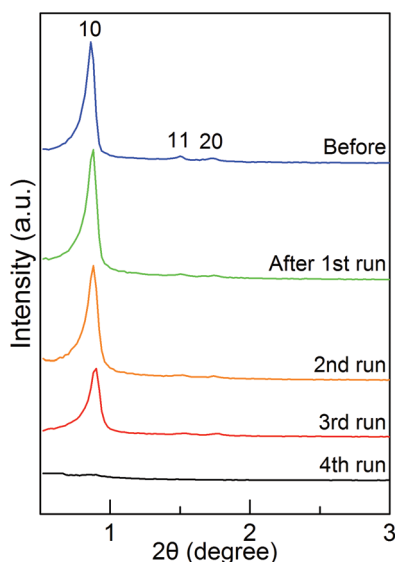


Fig. 6 PXRD patterns of Pd@M-SBA-15 before and after successive catalytic runs.

using a doubled amount of Pd@M-SBA-15 to catalyze the coupling reaction under optimal conditions for 1.5 h, filtering out the catalyst without cooling, and allowing the filtrate to react further. As shown in Fig. 5, without hot filtration, the yield of 4-acetobiphenyl continued to increase to 70% at a reaction time of 3 h and then to 90% at 9 h. If the catalyst was filtered at 1.5 h, the yield only slightly increased from 54% at 1.5 h to 64% at 3 h and remained almost constant afterwards. The results suggested that the leached Pd species in a very small amount were active for the Hiyama coupling but became inactive after reacting for a short period of time.

The other possible reason for the decreased product yield was the collapse of mesopores. This was indeed the case, as indicated by the decreased intensity of X-ray reflections of 2D-hexagonal structure after repeated uses. As shown in Fig. 6, no

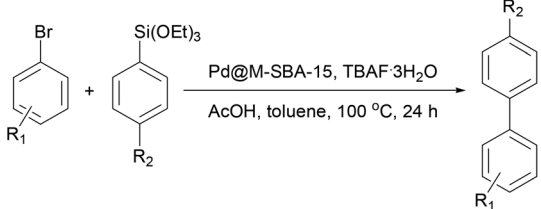
Table 2 The Hiyama cross-coupling of various aryl halides and phenyltriethoxysilane<sup>a</sup>

Entry	X	R	Yield <sup>b</sup> (%)
1	Br	4-Ac	92
2	Br	4-CN	71
3	Br	4-CHO	78
4	Br	4-Cl	81
5	Br	4-Me	73
6	Br	4-OMe	84
7	Cl	4-OMe	0
8	Cl	4-NO <sub>2</sub>	47
9	Br	2-CHO	75
10	Br	3-OMe	70
11 <sup>c</sup>	Br	Naphthalene	63
12	Br	2-OMe	13

<sup>a</sup> Reaction conditions: aryl halide (0.50 mmol), phenyltriethoxysilane (1.0 mmol), Pd@M-SBA-15 (0.5 mol%), AcOH (0.50 mmol), TBAF·3H<sub>2</sub>O (1.0 mmol), and toluene (3.0 mL) in air at 100 °C for 24 h. <sup>b</sup> Isolated yields. <sup>c</sup> 1-Bromonaphthalene.

reflection was observed in the PXRD pattern of Pd@M-SBA-15 after the fourth run. Obviously, even though the TMS groups (or TPS groups in Pd@P-SBA-15) on the mesopore surface could protect host silica from reacting with fluoride ions from TBAF·3H<sub>2</sub>O and/or AcOH and allow the catalyst to be recycled, the undesired reactions still took place slowly and inevitably after repeated uses of the catalysts. Therefore, we could conclude that a low level of Pd-leaching together with gradual collapse of mesopores of host silica caused the decrease in product yield for Pd@M-SBA-15 and Pd@P-SBA-15 after successive catalytic runs.

The substrate scope of the new cross-coupling protocol was examined under the optimal conditions using Pd@M-SBA-15 as a catalyst. As listed in Tables 2 and 3, in most cases, the Hiyama reactions of aryltriethoxysilanes with a variety of aryl halides afforded the corresponding biphenyl derivatives in good to excellent yields. Table 2 summarizes the results of the reactions of various aryl halides and phenyltriethoxysilane. Aryl bromides possessing either an electron-withdrawing (acetyl, cyano, formyl or chloro group, entries 1–4) or an electron-donating (methyl or methoxy group, entries 5 and 6) functionality at the *para*-position were found to be good substrates for the cross-coupling. We also tried the coupling reaction with aryl chlorides that are generally much less reactive than the corresponding bromides. Two chlorides, namely 4-chloroanisole and 4-nitrochlorobenzene, were tested in this study. Markedly, while 4-chloroanisole appeared to be a poor substrate (entry 7), a fairly good yield of 47% was obtained for 4-nitrochlorobenzene under the present reaction conditions (entry 8). The yield was much higher than that (7%) obtained

**Table 3** The Hiyama cross-coupling of various aryl bromides and aryltriethoxysilanes<sup>a</sup>


Entry	R <sub>1</sub>	R <sub>2</sub>	Yield <sup>b</sup> (%)
1	4-Ac	Cl	89
2	4-OMe	Cl	84
3	2-CHO	Cl	87
4	4-Ac	Me	79
5	4-OMe	Me	82
6	2-CHO	Me	38

<sup>a</sup> Reaction conditions: aryl bromide (0.50 mmol), aryltriethoxysilane (1.0 mmol), Pd@M-SBA-15 (0.5 mol%), AcOH (0.50 mmol), TBAF·3H<sub>2</sub>O (1.0 mmol), and toluene (3.0 mL) in air at 100 °C for 24 h. <sup>b</sup> Isolated yields.

using 5% Pd/C as a catalyst.<sup>42</sup> In addition to aryl bromides with functionalities at the *para*-position, Pd@M-SBA-15 could also catalyze the reactions with those having substituents at other positions that could be sterically hindered and gave decent yields (entries 9–11), with exceptions such as 2-bromoanisole (entry 12).

The cross-coupling protocol could also tolerate functional groups on the aryl ring of the aryltriethoxysilanes. As shown in Table 3, *p*-chlorotriethoxysilane was effectively coupled with 4-bromoacetophenone, 4-methoxybromobenzene and 2-bromobenzaldehyde to give the corresponding biphenyl derivatives in excellent yields (entries 1–3). When *p*-tolyltriethoxysilane was used as a reactant, slightly lower yields were obtained for the coupling with *para*-substituted bromobenzenes and only 38% isolated yield was obtained for the reaction with 2-bromobenzaldehyde. The results seemed to suggest possible electronic effects of the substituent group in aryltriethoxysilanes on the efficiency of the cross-coupling reaction. In addition, the steric factor seemed to become more pronounced for the substituted aryltriethoxysilanes and should also be considered for the present cross-coupling system.

## Conclusions

Pd catalysts containing Pd nanoparticles preferentially deposited in the micropores of the SBA-15 with hydrophobic groups grafted on mesopores have been prepared. They exhibited excellent catalytic activities for the ligand-free Hiyama cross-coupling between various aryltriethoxysilanes and aryl halides under relatively mild reaction conditions. The catalysts could be reused, and the decreased catalytic activity was attributed to a low level of Pd-leaching and gradual collapse of

mesopores of host silica after successive catalytic runs. The protocol using the designed catalysts provides an economical synthetic method for the construction of biphenyl derivatives.

## Acknowledgements

The authors thank the National Science Council of the Republic of China for financial support under contract no. NSC 101-2811-M-007-089 and NSC 101-2628-M-007-001-MY2.

## References

- 1 T. Hiyama and E. Shirakawa, in *Handbook of Organopalladium Chemistry for Organic Synthesis*, ed. E. Negishi and A. de Meijere, Wiley Interscience, New York, 2002, vol. 1, p. 285.
- 2 S. E. Denmark and R. F. Sweis, *Acc. Chem. Res.*, 2002, **35**, 835.
- 3 C. J. Handy, A. S. Manoso, W. T. McElroy, W. M. Seaganish and P. DeShong, *Tetrahedron*, 2005, **61**, 12201.
- 4 S. E. Denmark and J. H. C. Liu, *Angew. Chem., Int. Ed.*, 2010, **49**, 2978.
- 5 H. F. Sore, W. R. J. D. Galloway and D. R. Spring, *Chem. Soc. Rev.*, 2012, **41**, 1845.
- 6 Y. Nakao and T. Hiyama, *Chem. Soc. Rev.*, 2011, **40**, 4893.
- 7 J. Y. Lee and G. C. Fu, *J. Am. Chem. Soc.*, 2003, **125**, 5616.
- 8 P. Pierrat, P. Gros and Y. Fort, *Org. Lett.*, 2005, **7**, 697.
- 9 J. Ju, H. Nam, H. M. Jung and S. Lee, *Tetrahedron Lett.*, 2006, **47**, 8673.
- 10 I. Gordillo, E. de Jesús and C. López-Mardomingo, *Org. Lett.*, 2006, **8**, 3517.
- 11 I. Dorado, R. Andres, E. de Jesus and J. C. Flores, *J. Organomet. Chem.*, 2008, **693**, 2147.
- 12 L. Zhang and J. Wu, *J. Am. Chem. Soc.*, 2008, **130**, 12250.
- 13 C. M. So, H. W. Lee, C. P. Lau and F. Y. Kwong, *Org. Lett.*, 2009, **11**, 317.
- 14 I. Blaszczyk and A. M. Trzeciak, *Tetrahedron*, 2010, **66**, 9502.
- 15 S. M. Raders, J. V. Kingston and J. G. Verkade, *J. Org. Chem.*, 2010, **75**, 1744.
- 16 A. Komáromi, F. Szabó and Z. Novák, *Tetrahedron Lett.*, 2010, **51**, 5411.
- 17 A. Pal, R. Ghosh, N. N. Adarsh and A. Sarkar, *Tetrahedron*, 2010, **66**, 5451.
- 18 A. Skarzynska and A. Gniewek, *J. Organomet. Chem.*, 2011, **696**, 2985.
- 19 D. C. Blakemore and L. A. Marples, *Tetrahedron Lett.*, 2011, **52**, 4192.
- 20 G. A. Molander and L. Iannazzo, *J. Org. Chem.*, 2011, **76**, 9182.
- 21 T. Huang and C. J. Li, *Tetrahedron Lett.*, 2002, **43**, 403.
- 22 J. H. Li, C. L. Deng, W. J. Liu and Y. X. Xie, *Synthesis*, 2005, 3039.
- 23 E. Alacid and C. Nájera, *Adv. Synth. Catal.*, 2006, **348**, 945.

- 24 T. Mino, Y. Shirae, T. Saito, M. Sakamoto and T. Fujita, *J. Org. Chem.*, 2006, **71**, 9499.
- 25 S. Shi and Y. Zhang, *J. Org. Chem.*, 2007, **72**, 5927.
- 26 Á. Gordillo, E. de Jesús and C. López-Mardomingo, *Chem. Commun.*, 2007, 4056.
- 27 D. Srimani, S. Sawoo and A. Sarkar, *Org. Lett.*, 2007, **9**, 3639.
- 28 R. Dey, K. Chattopadhyay and B. C. Ranu, *J. Org. Chem.*, 2008, **73**, 9461.
- 29 B. C. Ranu, R. Dey and K. Chattopadhyay, *Tetrahedron Lett.*, 2008, **49**, 3430.
- 30 S. N. Chen, W. Y. Wu and F. Y. Tsai, *Tetrahedron*, 2008, **64**, 8164.
- 31 C. Pan, M. Liu, L. Zhao, H. Wu, J. Ding and J. Cheng, *Catal. Commun.*, 2008, **9**, 1685.
- 32 D. Alonso and C. Nájera, *Chem. Soc. Rev.*, 2010, **39**, 2891.
- 33 G. C. Fortman and S. P. Nolan, *Chem. Soc. Rev.*, 2011, **40**, 5151.
- 34 A. Kumar and P. Ghosh, *Eur. J. Inorg. Chem.*, 2012, **2012**, 3955.
- 35 F. Kong, C. Zhou, J. Wang, Z. Yu and R. Wang, *Chem-PlusChem*, 2013, **78**, 536.
- 36 C. Premi and N. Jain, *Eur. J. Org. Chem.*, 2013, 5493.
- 37 L. Duran Pachon, M. B. Thathagar, F. Hartl and G. Rothenberg, *Phys. Chem. Chem. Phys.*, 2006, **8**, 151.
- 38 J. Y. Kim, Y. Jo, S. K. Kook, S. Lee and H. C. Choi, *J. Mol. Catal. A: Chem.*, 2010, **323**, 28.
- 39 B. Sreedhar, A. S. Kumar and D. Yada, *Synlett*, 2011, 1081.
- 40 T. Borkowski, P. Subik, A. M. Trzeciak and S. Wolowiec, *Molecules*, 2011, **16**, 427.
- 41 V. K. R. Kumar, S. Krishnakumar and K. R. Gopidas, *Eur. J. Org. Chem.*, 2012, 3447.
- 42 T. Yanase, Y. Monguchi and H. Sajiki, *RSC Adv.*, 2012, **2**, 590.
- 43 D. Shah and H. Kaur, *J. Mol. Catal. A: Chem.*, 2012, **359**, 69.
- 44 C. Diebold, A. Derible, J. M. Becht and C. Le Drian, *Tetrahedron*, 2013, **69**, 264.
- 45 A. P. Kumar, B. P. Kumar, A. B. V. K. Kumar, B. T. Huy and Y. I. Lee, *Appl. Surf. Sci.*, 2013, **265**, 500.
- 46 A. Grirrane, H. Garcia and A. Corma, *J. Catal.*, 2013, **302**, 49.
- 47 J. Guerra and M. A. Herrero, *Nanoscale*, 2010, **2**, 1390.
- 48 I. Favier, D. Madec, E. Teuma and M. Gomez, *Curr. Org. Chem.*, 2011, **15**, 3127.
- 49 A. Balanta, C. Godard and C. Claver, *Chem. Soc. Rev.*, 2011, **40**, 4973.
- 50 S. K. Beaumont, *J. Chem. Technol. Biotechnol.*, 2012, **87**, 595.
- 51 P. Taladriz-Blanco, P. Hervés and J. Pérez-Juste, *Top. Catal.*, 2013, **56**, 1154.
- 52 D. Zhao, J. Feng, Q. Huo, N. Melosh, G. H. Fredrickson, B. F. Chmelka and G. D. Stucky, *Science*, 1998, **279**, 548.
- 53 D. Zhao, Q. Huo, J. Feng, B. F. Chmelka and G. D. Stucky, *J. Am. Chem. Soc.*, 1998, **120**, 6024.
- 54 M. Impéror-Clerc, P. Davidson and A. Davidson, *J. Am. Chem. Soc.*, 2000, **122**, 11925.
- 55 A. Galarneau, H. Cambon, F. Di Renzo, R. Ryoo, M. Choi and F. Fajula, *New J. Chem.*, 2003, **27**, 73.
- 56 C. M. Yang, B. Zibrowius, W. Schmidt and F. Schüth, *Chem. Mater.*, 2003, **15**, 3739.
- 57 C. M. Yang, B. Zibrowius, W. Schmidt and F. Schüth, *Chem. Mater.*, 2004, **16**, 2918.
- 58 R. Palkovits, C. M. Yang, S. Olejnik and F. Schüth, *J. Catal.*, 2006, **243**, 93–98.
- 59 C. M. Yang, H. A. Lin, B. Zibrowius, B. Spliethoff, F. Schüth, S. C. Liou, M. W. Chu and C. H. Chen, *Chem. Mater.*, 2007, **19**, 3205.
- 60 H. A. Lin, C. H. Liu, W. C. Huang, S. C. Lion, M. W. Chu, C. H. Chen, J. F. Lee and C. M. Yang, *Chem. Mater.*, 2008, **20**, 6617.
- 61 C. H. Liu, Y. Guan, E. J. M. Hensen, J. F. Lee and C. M. Yang, *J. Catal.*, 2011, **282**, 94.
- 62 C. H. Liu, N. C. Lai, S. C. Liou, M. W. Chu, C. H. Chen and C. M. Yang, *Microporous Mesoporous Mater.*, 2013, **179**, 40.
- 63 E. J. Milton, J. A. Fuentes and M. L. Clarke, *Org. Biomol. Chem.*, 2009, **7**, 2645.
- 64 M. Lalonde and T. H. Chan, *Synthesis*, 1985, 817.